COPERNICUS MASTER IN DIGITAL EARTH

PARIS LODRON UNIVERSITÄT SALZBURG

Biophysical Parameters for Urban Heat Island Analysis

A Comparison of Satellite-Derived LST and Spectral Indices with High-Resolution Thermal Data in Klagenfurt

Analysis and Modeling (Remote Sensing)

Supervisor: Hannah Augustin

Annabelle Kiefer (s1111172)

Due date: 17/08/2025

Contents

List of figures 1
List of abbreviations 2
Abstract 2
Introduction 3
Data and Methods 5
Study Area 6
Data and Pre-Processing 7
Methods 8
Deriving spectral indices & LULC classification 8
Identification of UHIs in Klagenfurt 9
Results 9
Landsat-derived Spectral Indices and LST 10
Landsat-based UHI Mapping at Small and Large Spatial Scale 12
Comparing Landsat-based and High-resolution UHI Mapping 14
Discussion 15
Limitations 15
Landsat-derived Spectral Indices and LST 16
Landsat-based UHI Mapping at Small and Large Spatial Scale 17
Comparing Landsat-based and High-resolution UHI Mapping 18
Conclusion 18
References & Acknowledgements 19

List of figures

Figure 1. Flowchart illustrating the entire workflow (created with draw.io). 6
Figure 2. Climate data for Klagenfurt on August 11, 2024 (Meteosat, 2025).. 7
Figure 3. NDVI, SAVI, NDBI & IBI for Klagenfurt. 10
Figure 4. Regression Analysis between LST & the corresponding spectral index 11
Figure 5. Land Use Classification (vegetation & urban areas) 12
Figure 6. Identification of UHIs based on equation 5. 13
Figure 7. UHI Identification for urban areas only, based on equation 6. 13
Figure 8. Identification of UHIs based on normalized LST. 14
Figure 9. Comparison of UHI identification based on Landsat and high-resolution data. 15
Figure 10. Comparison of UHI identification with high-resolution data during the day and night. 15

List of abbreviations

ARD: Analysis Ready Data
ASTER: Advanced Spaceborne Thermal Emission and Reflection Radiometer
CEOS: Committee on Earth Observation Satellite
DI: Disturbance Index
DN: Digital Numbers
EROS: Earth Resources Observation and Science (Center)
IBI: Index-based Built-up Index
LST: Land Surface Temperature
LULC: Land Use/Land Cover
MNDWI: Modified Normalized Difference Water Index
NDBI: Normalized Difference Built-up Index
NDVI: Normalized Difference Vegetation Index
OLI: Operational Land Image
PROMETHEUS: Progressive methods of thermal high-resolution earth surveillance for urban sustainability
SAVI: Soil-Adjusted Vegetation Index
SUHI: Surface Urban Heat Island
TIRS: Thermal Infrared Sensor
TOA: Top of Atmosphere (Reflectance)
UHI: Urban Heat Island
UTFVI: Urban Thermal Field Variance Index

Abstract

This study aims to investigate the distribution of Urban Heat Islands (UHIs) in Klagenfurt, Austria using medium-resolution Landsat 9 data as well as high-resolution thermal data. The data was acquired in August 2024 and thus represents a hot summer day, which can provide valuable insights into the formation of UHIs. In general, UHIs were identified using Landsat 9 Land Surface Temperature (LST), spectral indices and high-resolution thermal data. To better distinguish UHIs from non-UHIs, Land Use/Land Cover (LULC) classes were defined based on spectral indices. Moreover, equations based on the normalized LST, the mean LST and its standard deviation were formed to identify UHIs. Since two datasets with different spatial resolution were used, the results were also compared to determine which datasets and methods are most efficient for identifying UHIs in Klagenfurt.

The calculated spectral indices efficiently show the distribution between urban areas and vegetation in Klagenfurt. At the same time, a strong correlation was found between spectral indices and LST. While a strong negative correlation was found between LST and vegetation biophysical indices, the correlation between LST and urban biophysical indices is positive. The results of the UHI identification show a strong accumulation of UHIs in the city center, whereas the surroundings of Klagenfurt have a cooling

effect. The best distinction between UHIs and non-UHIs was found at the city level for the high-resolution thermal dataset, while a combination of the urban LULC class and Landsat 9 LST also helped to better differentiate UHIs from cooler areas in the city center.

Introduction

Urbanization is accelerating rapidly, with more than half of the world's population now living in urban areas (Ritchie et al., 2024). This leads to numerous challenges in urban areas, which are often exacerbated by the ongoing climate change. One of these challenges is the formation of Urban Heat Islands (UHIs), which are urban areas with higher surface temperatures compared to surrounding rural areas (Almeida et al., 2021). They are driven by surface properties, with built-up areas generally accelerating UHI dynamics, whereas green spaces and water bodies can have a positive influence on the microclimate (Guha et al., 2018). In urban agglomerations, certain building materials that absorb solar radiation contribute in particular to the formation of UHIs (Almeida et al, 2021). This formation can have an impact on both humans and nature. Especially vulnerable groups are exposed to serious health risks or thermal discomfort in general (Sangiorgio et al., 2020; Almeida et al., 2021). At the same time, especially the hydrological conditions can be adversely affected by UHIs, for example in the form of a reduction in water bodies (Almeida et al., 2021).

Due to the importance of the topic, the number of publications on the identification of UHIs using remote sensing techniques has increased over the past 20 years (Almeida et al., 2021). Remote sensing here has the advantage of offering extensive spatial coverage and high temporal resolution (Zhou et al., 2018). In the context of UHI identification, Land Surface Temperature (LST) estimation is the most commonly used method. Unlike measurements taken by metrological stations a few meters above the ground, LST directly indicates the surface temperature (Almeida et al., 2021). For this reason, Surface Urban Heat Island (SUHI) is the technical term for UHIs derived from LST. However, for simplicity and consistency, the term UHI is used as a synonym in this article, as is common in similar studies. In general, Landsat products are most commonly used for LST retrieval, although MODIS data or Sentinel 3 could also be used (Almeida et al., 2021). For Landsat 8 and 9, several algorithms have been developed to retrieve LST from the thermal infrared bands, such as the radiative transfer equation algorithm, the single window algorithm and the split window algorithm, which are generally based on the Planck blackbody radiation formula (Meng et al., 2021). Alternatively, the surface temperature of Landsat Collection 2 Level-2 can be used, which is analysis ready data (ARD) that has already been retrieved based on generalized emissivity and NDVI, among other factors (EROS Center, 2020).

In addition to LST, biophysical parameters are often used for Land Use/Land Cover (LULC) Classification, which can contribute to understanding UHI dynamics and developing strategies to mitigate them (Almeida et al., 2021). Here, land use has a strong influence on LST, which is why biophysical indices can be used to gain insights into the distribution of LST (Mushore et al., 2022). There are a variety of biophysical indices, but for the analysis of UHIs, vegetation biophysical indices and urban biophysical indices play a particularly important role. The spectral index most commonly used in the context of UHI analysis is the Normalized Difference Vegetation Index (NDVI) which provides important insights into the distribution of vegetated areas (Almeida et al, 2021). In contrast, the Normalized Difference Built-up Index (NDBI) is often used to quantify the extent of urban areas. In this context, the correlation between spectral indices and LST has also been extensively studied. Here, vegetation biophysical indices show a strong negative correlation with LST, whereas urban biophysical indices generally correlate positively with LST (Guechi et al., 2021).

As mentioned above, there are numerous studies that use various remote sensing methods and data sources to identify UHIs in different study areas and spatial scales. Although these studies have been conducted worldwide, there is a concentration on the Asian continent, whereas fewer studies have been carried out in Europe (Almeida et al., 2021). In Europe, these studies often focus on Mediterranean regions with hotter climates. For example, *Guha* et al. (2018) analyzed LST with NDVI and NDBI using Landsat 8 data in Florence and Naples, Italy, identifying several UHIs within city limits as well as a strong correlation between LST and NDVI (negative) and NDBI (positive). Another study by *Aslan and Koc-San* (2021) investigated the magnitude of SUHIs in Bursa, Turkey, over an 11-year period using Landsat LST as well as a series of spectral indices to analyze LULC. They found that spectral indices such as NDVI can be used efficiently to distinguish between urban and vegetated areas for SUHI studies (Aslan & Koc-San, 2021). *Bečić and Pažur* (2025) investigated the spatial patterns of UHIs in Zagreb, Croatia, using a statistical approach in R with Landsat 9 LST and urban spatial planning documents. As part of their study, they used Exploratory Spatial Data Analysis, regression models and spatial autocorrelation to identify clusters of UHIs and their dependencies on land use (Bečić and Pažur, 2025).

Currently, there is a lack of research on medium-sized European cities that are not located in the Mediterranean region, so further investigation into the distribution of UHIs in these cities is needed. At the same time, a research gap exists for comparing medium-resolution open data, such as Landsat, with high-resolution thermal aerial imagery. In Klagenfurt am Wörthersee, a medium-sized European city in southern Austria, a project called PROMETHEUS (Progressive methods of thermal high-resolution earth surveillance for urban sustainability) is currently underway between the Paris Lodron University Salzburg and the city. The interdisciplinary project, which runs from June 2024 to May 2026,

aims to use high-resolution thermal data and artificial intelligence to derive data which can be used for evidence-driven climate adaptation strategies in Klagenfurt (FFG, 2024). The acquired high-resolution thermal data was kindly made available for use in the following analysis. Therefore, this study aims to identify UHIs in Klagenfurt using Landsat data and high-resolution thermal data. For the Landsat data, spectral indices are first calculated and then used to better derive UHIs with LST in Klagenfurt on two different spatial scales. The results are then compared with the UHIs identified using the high-resolution thermal data which was acquired as part of the PROMETHEUS project. This leads to the following research questions.

1. How effective is a combined approach of using Landsat-derived biophysical spectral indices and Land Surface Temperature (LST) for identifying Urban Heat Islands (UHIs) in Klagenfurt?
2. How well does the identification of UHIs perform with Landsat data compared to the results obtained with high-resolution thermal data?
3. How does the performance vary when applied at different spatial scales such as to the entire urban area or with a focus on the city center?

Data and Methods

For the UHI analysis in Klagenfurt, Landsat 9 Surface Reflectance & Surface Temperature data from August 11, 2024, were used and compared with high-resolution thermal data from August 11, 2024. The Landsat data was first preprocessed by stacking the relevant bands and applying scaling factors. Subsequently, both the Landsat data as well as the high-resolution thermal images were cropped for large-scale and small-scale analysis.

Whereas the high-resolution thermal images were immediately used to normalize the LST and identify UHIs based on LST, spectral indices were first calculated for the Landsat Surface Reflectance data. These spectral indices served as input for a coarse LULC classification, which was used to better understand the distribution of LST in urban and vegetated areas. The Landsat results of LST normalization and UHI identification were then compared with the results of the high-resolution thermal data.

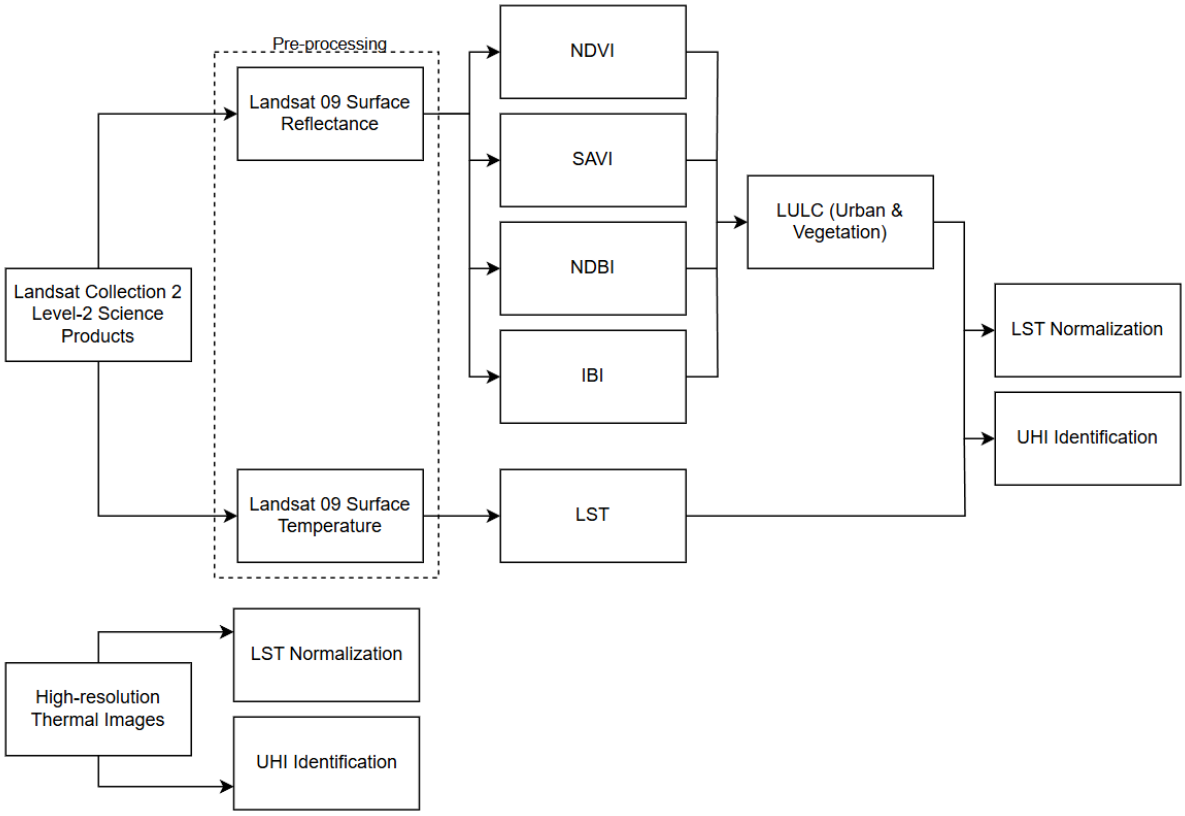

Figure 1. Flowchart illustrating the entire workflow (created with draw.io).

Study Area

Klagenfurt am Wörthersee is a medium-sized European city in southern Austria in the federal state of Carinthia. As the name of the city suggests, Klagenfurt borders lake Wörthersee, the warmest lake in the European alps, to the west (Magistrat der Landeshauptstadt Klagenfurt am Wörthersee, 2025). Accordingly, both the lake and the geographical location in a valley surrounded by the Alps have a major influence on the local climate. In general, the average annual temperature in Klagenfurt is 9°C and the annual precipitation is around 1332 mm (Climate-Data.org, 2025). August is usually one of the hottest months, with an average temperature of around 19°C (Climate-Data.org, 2025). This also applies to August 11, 2024, when both the Landsat data as well as the high-resolution thermal data were acquired. On this day, the average temperature was 25.4°C and there was no precipitation. The temperature began to rise in the morning and reached a high of 32°C at around 5 p.m. (Meteosat, 2025). This information is important when comparing the exact time of acquisition, which was around 12 a.m. for the Landsat image and between 2 and 3 p.m. for the high-resolution thermal image. Correspondingly, both images were captured during a period of high temperature, with the temperature for the high-resolution thermal image possibly being a few degrees higher than the Landsat image.

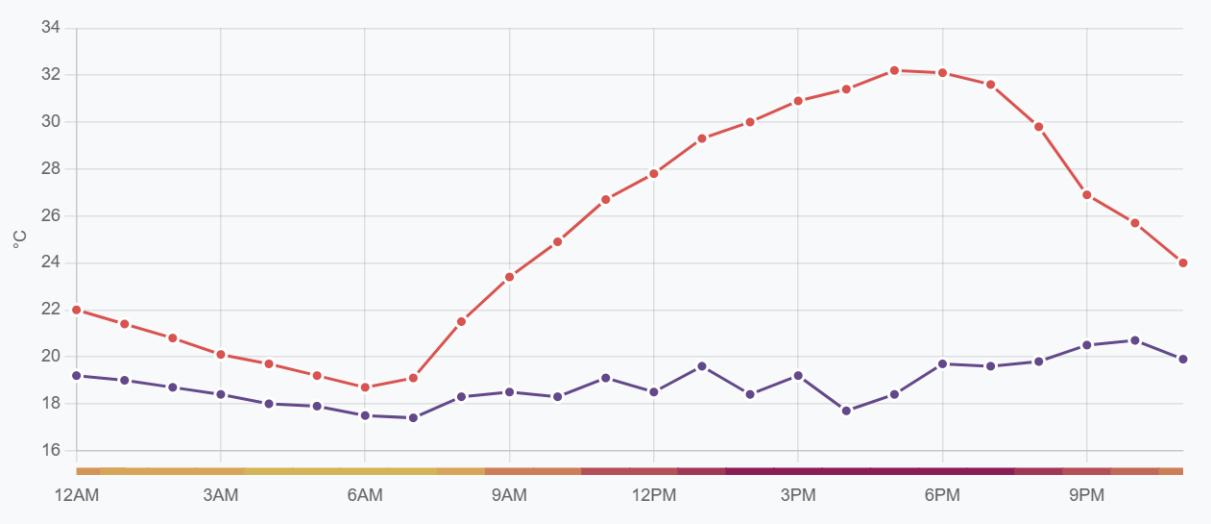

Figure 2. Climate data for Klagenfurt on August 11, 2024 (Meteosat, 2025). The red line shows the temperature and the blue line shows the dew point.

Data and Pre-Processing

For this analysis, Landsat 9 Operational Land Image (OLI) / Thermal Infrared Sensor (TIRS) Collection 2 Level-2 data was acquired for August 11, 2024 via EarthExplorer. The spectral bands of Landsat 9 have a spatial resolution of 30m and the thermal bands of 100m. Additionally, high-resolution thermal data with a spatial resolution of 1m, acquired on August 11, 2024, during a thermal flight, was provided for analysis. At this point, it should be noted that the high-resolution thermal data has not yet been calibrated, which leads to problems with the local projection and unrealistic LST values for metallic surfaces. For this reason, this dataset was mainly used for visual comparison of the LST values with the results generated from the Landsat data.

The Landsat data products used are analysis ready data (ARD) as defined by the Committee on Earth Observation Satellites (CEOS), which means that the data has already been processed to a minimum set of requirements (EROS Center, 2020). In this case, the surface reflectance data has already been atmospherically corrected. Similarly, the surface temperature data has been corrected using top-of-atmosphere (TOA) reflectance, data from the Advanced Spaceborne Thermal Emission and Reflection Radiometer (ASTER) Global Emissivity Database and ASTER NDVI data. At the same time, the surface temperature data was resampled to a spatial resolution of 30m (EROS Center, 2020).

To correctly interpret the Surface Reflectance and Surface Temperature data, scaling factors defined by the Earth Resources Observation and Science (EROS) Center had to be applied to the relevant bands. These convert digital numbers (DNs) into reflectance values or temperature values in Kelvin (EROS Center, 2020). Since the surface temperature is given in Kelvin, the thermal band was converted to Celsius to better compare the LST with the high-resolution thermal data. In this context, it should be

mentioned that although Landsat 9 has two thermal infrared bands, only band 10 was used due to its higher accuracy, as recommended in the literature (Mushore et al., 2022). At the same time, it should be noted that due to the use of Landsat Collection 2 Level-2 data, the LST was not calculated manually as is common in literature.

In general, the acquisition date shows low cloud cover of less than 2%, which is important to avoid cloud and shadow effects that cause problems when analyzing surface reflectance and temperature (Mushore et al., 2022). Especially thermal sensors often do not provide reliable outputs when clouds are present (Almeida et al., 2021). Although cloud cover was low during this acquisition, problems with high spectral differences arose during the creation of the spectral indices, which is why clouds, cloud shadows and water had to be manually masked using the quality assessment band. The bands were then stacked and cropped to the predefined extents of Klagenfurt, representing both a larger and smaller area. This last step was repeated with the high-resolution thermal data to ensure accurate comparisons.

Methods

The analysis was performed in R, making it easily reproducible and interoperable with different datasets, scales and study areas. In general, the methods differ between the two data sources, Landsat 9 and high-resolution thermal data. For the Landsat data, vegetation and urban biophysical indices were first derived and then used to create LULC classes. Subsequently, UHIs were detected using LST and defined LULC classes. For the high-resolution thermal data, the same equations were used to identify UHIs, but without further differentiation based on LULC classes.

All code used in this study is openly available on GitHub at https://github.com/annabellekiefer/uhi_analysis_klagenfurt.git.

Deriving spectral indices & LULC classification

For this analysis, specific vegetation and urban biophysical indices were derived to identify LULC classes that can contribute to the identification of UHIs. Although a variety of different spectral indices are available, a set of two vegetation and two urban biophysical indices commonly used in UHI analysis was selected for this purpose. The first is the Normalized Difference Vegetation Index (NDVI), a commonly used vegetation index based on the ratio between the red and near-infrared channels (Rouse et al., 1973). In addition, the Soil-Adjusted Vegetation Index (SAVI), first introduced by *Huete* (1988), was used in this context because it is frequently used in urban areas (Aslan & Koc-San, 2021). SAVI uses a soil-adjusted correction factor that allows vegetation to be detected even in less densely vegetated areas. To detect urban areas in the test area, the Normalized Difference Built-up Index (NDBI) was derived using the shortwave-infrared and near-infrared bands (Zha et al., 2003). Lastly, the Index-

based Built-up Index (IBI) was calculated, which is used for rapid detection of urban areas while suppressing background noises. It is based on the spectral indices NDVI, NDBI and Modified Normalized Difference Water Index (MNDWI) (Xu, 2008).

The formulas for the vegetation and urban biophysical indices are as follows.

(1) $NDVI = \frac{(NIR-Red)}{(NIR+Red)}$

(2) $SAVI = \frac{(NIR-Red)(1+l)}{(NIR+Red+l)}$ *(the soil-adjusted correction factor l varies from 0 (very dense vegetation) to 1 (very sparse vegetation) and is generally accepted to be 0.5)*

(3) $NDBI = \frac{(SWIR-NIR)}{(SWIR+NIR)}$

(4) $IBI = \frac{2SWIR/(SWIR+NIR)-[NIR/(NIR+Red)+Green/(Green+SWIR)]}{2SWIR/(SWIR+NIR)+[NIR/(NIR+Red)+Green/(Green+SWIR)]}$

The indices are usually strongly correlated with LST, which is why they are often used to identify LULC classes. For this purpose, thresholds were defined based on suggestions from literature, but also by trial and error and visualization of the histograms. In this context, the use of more than one spectral index helped to better identify the two LULC classes urban areas and vegetation. Vegetation was defined here as areas with NDVI values above 0.4 and SAVI values above 0.3. The thresholds for the urban LULC category were NDVI below 0.4, SAVI below 0.3, NDBI above -0.25 and IBI above -0.2.

Identification of UHIs in Klagenfurt

UHIs in Klagenfurt were identified for two different scales and at two spatial resolutions using Landsat 9 LST and high-resolution thermal data. Here, two approaches were used. First, UHIs were defined as areas where LST is above a custom threshold, using the mean LST and its standard deviation (Ma et al., 2009; Guha et al., 2018). This equation was used for both scales as well as resolutions.

(5) $UHI = LST > (LSTmean + 0.5 * LSTstd)$

Additionally, LST was normalized and then categorized into UHIs and non-UHIs. Here, areas with temperatures above 1.5°C or 2°C are identified as UHIs (Aslan & Koc-San, 2021).

(6) $UHI = \frac{(LST-LSTmean)}{LSTstd}$

Results

The results section is based on the methodology, which is why the Landsat-derived spectral indices and LST are presented first, followed by Landsat-based UHI mapping at a small and large spatial scale and a comparison between Landsat-based and high-resolution UHI mapping.

Landsat-derived Spectral Indices and LST

The two vegetation indices clearly show the distribution of urban areas in blue in the center and vegetated areas in green or yellow in the vicinity of Klagenfurt. Here, high values indicate vegetation, while lower values show urban areas. When comparing NDVI and SAVI, the advantages of SAVI become clear. While the vegetated areas in the NDVI image show similar values overall, SAVI distinguishes much better between different types of vegetation, with densely vegetated areas shown in yellow. Additionally, the values of NDVI and SAVI have different scales. At this point, it should also be noted that the masked areas in the images are clearly visible and are here shown as white areas.

In contrast, the two urban biophysical indices show the opposite distribution, with high values representing urban areas and lower values showing vegetated areas. Both indices clearly show the city center of Klagenfurt with its relatively densely built-up areas. At the same time, similar to the vegetation biophysical indices, bare soil is also considered as built-up. This varies slightly when comparing NDBI and IBI, although the differentiation between urban and vegetation looks rather similar. Nevertheless, the value ranges are quite different, which is why using a combination of both indices is helpful in identifying LULC classes.

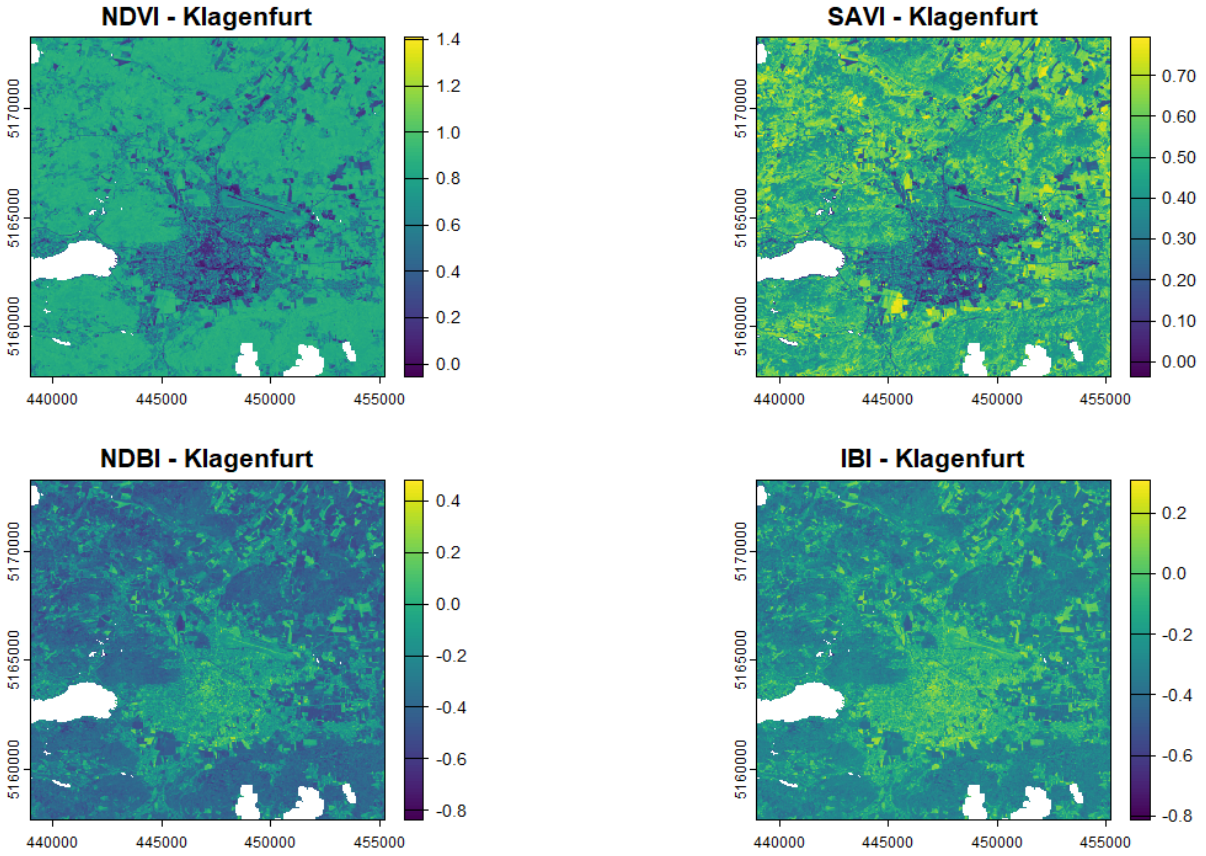

Figure 3. NDVI, SAVI, NDBI & IBI for Klagenfurt.

As mentioned earlier, the specific set of spectral indices was selected because they correlate with LST and can therefore be used efficiently to define LULC classes prior to the identification of UHIs. When comparing the regression plots of the four indices on the larger extent, there is a negative correlation between LST, NDVI and SAVI whereas NDBI and IBI have a positive correlation with LST. In all four graphs, the p-value is below $2.2e^{-16}$, indicating a strong correlation. At the same time, the regression coefficient is relatively high for all diagrams, although the highest correlation was found between IBI and LST with 0.669. SAVI, on the other hand, had the lowest coefficient with 0.5248, where especially temperatures between 25°C and 30°C cover a wide range of SAVI values between 0.4 and 0.7.

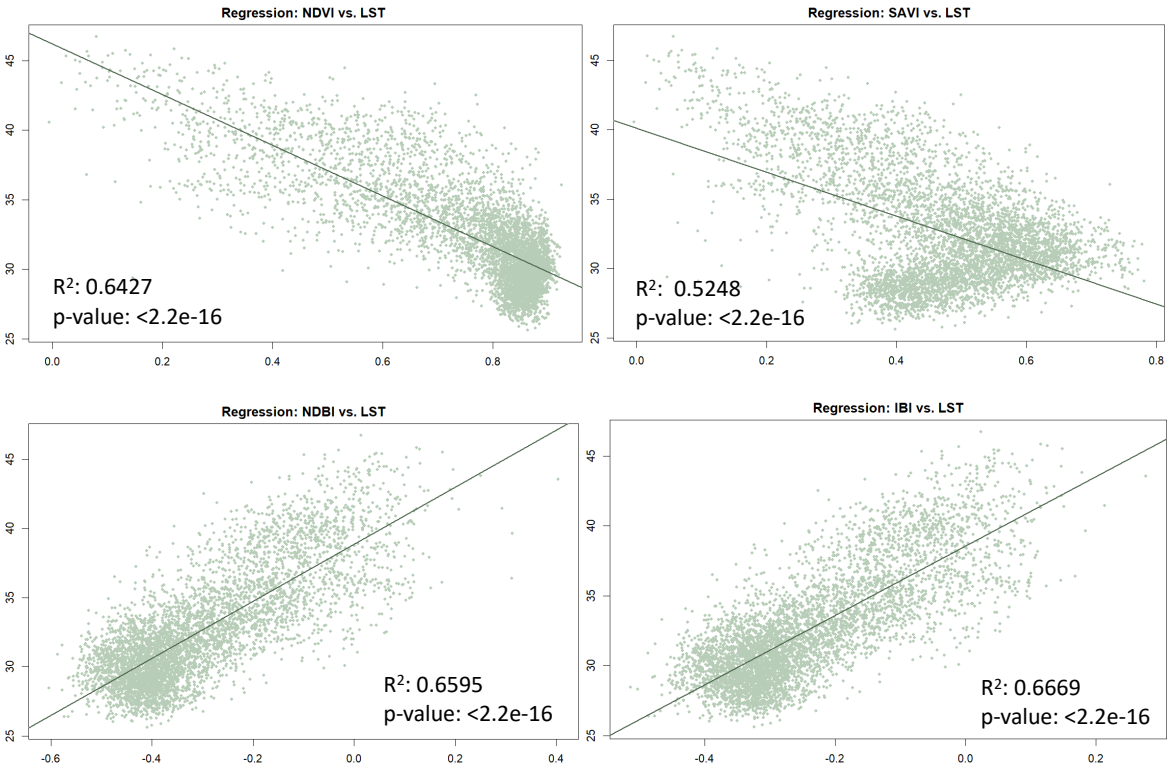

Figure 4. Regression analysis between LST & the corresponding spectral index (NDVI, SAVI, NDBI, IBI).

The resulting land use classification clearly distinguishes between urban areas and vegetation. Similar to the distribution determined using spectral indices, urban areas are located in the center, whereas areas surrounding Klagenfurt are mainly characterized by vegetation. Since water and other interfering factors such as clouds had to be masked, these areas appear as gray and are defined in the LULC class *other*. Similarly, some areas that could not be clearly assigned to the LULC class *urban* or *vegetation* using the thresholds are now displayed in the *other* class. These areas consist partly of bare soil, which is often difficult to distinguish from urban areas.

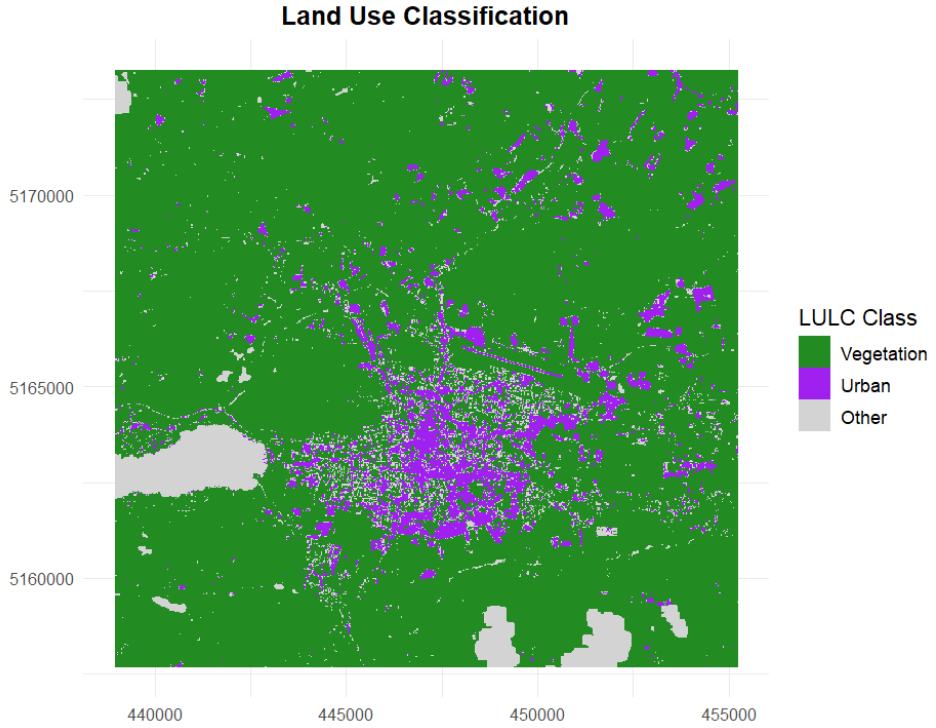

Figure 5. Land Use Classification (vegetation & urban areas) based on thresholds of spectral indices.

Landsat-based UHI Mapping at Small and Large Spatial Scale

Two different methods were used to identify UHIs in Klagenfurt. At the same time, the analysis was carried out on two scales to find out where the most meaningful results could be obtained. Here, the study area covers either the city center of Klagenfurt or the entire surrounding area with abundant vegetation in addition to the urban areas.

First, a threshold value based on the mean LST in the area and the standard deviation was used to define UHIs. For the large test area, the distribution between the city center with many urban areas and its surroundings with many green areas is particularly noticeable. At the same time, some harvested agricultural fields and bare soil are also identified as UHIs. It also becomes clear that at this scale, no distinction can be made between warmer and colder areas in the city center, as the entire area becomes one large UHI. The analysis for the smaller test area, on the other hand, helps to distinguish UHIs in the city center more efficiently. Here, some hotspots become visible for the first time such as the area around the airport in the north. In this extent, some green spaces with cooler temperatures can also be identified in the city center.

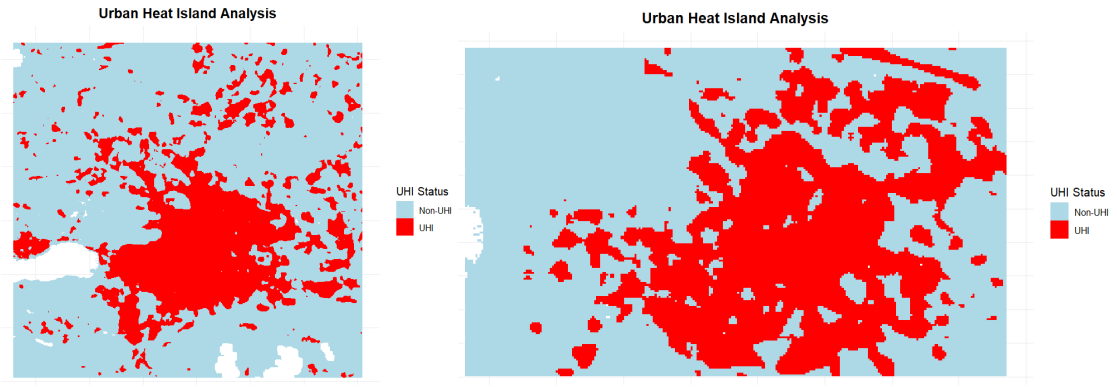

Figure 6. Identification of UHIs based on equation 5.

To better distinguish UHIs in the city center from cooler areas, the urban mask from the LULC classification based on the thresholds of the spectral indices was applied. This method allows UHIs to be better distinguished from non-UHIs on both scales. In the larger extent, it becomes clear that the city center is hotter than the surrounding agricultural areas and bare soil, which are now identified as non-UHIs rather than UHIs. In the smaller extent, certain urban areas in the city center become strong UHIs, while other areas appear cooler. At this point, the limitations and contradictions of this approach must also be mentioned, as the results vary, especially for the two scales. An example of this is the airport, which appears as an UHI in the larger extent, while in the smaller extent it becomes a non-UHI.

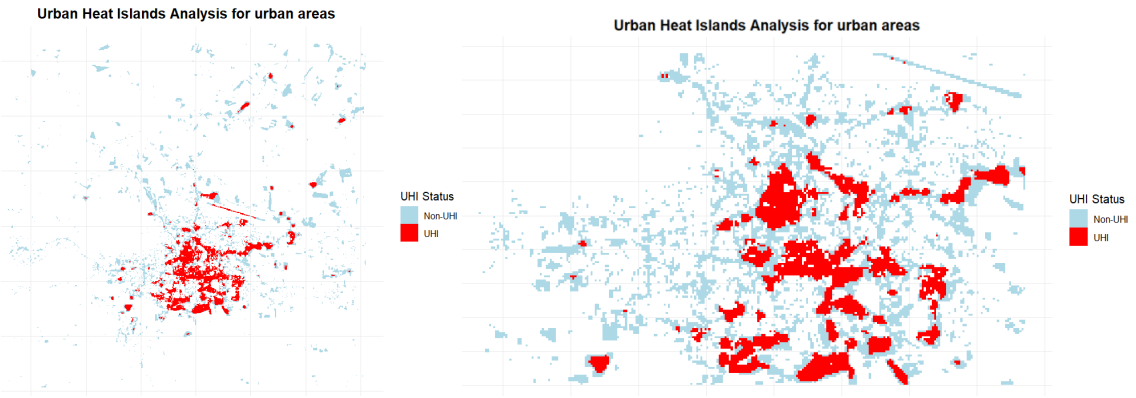

Figure 7. UHI Identification for urban areas only based on equation 6.

As a second approach, the LST was standardized and UHIs were identified as areas where the standardized LST is greater than 1.5°C or 2°C. Especially with the larger extent, this also helps to distinguish extremely hot urban areas from cooler ones. With this approach, the city center does not appear as one large UHI, but is divided into more extreme UHIs in dark red and less extreme ones in red. Due to the normalization of the LST, bare soil is now rarely classified as UHIs, but instead the focus is strongly on urban areas. For the smaller extent, on the other hand, the results appear less informative at first glance, as only a few areas were identified as UHIs. Similar to the first approach, these results could still be very useful, as they might be the best way to identify the hottest areas in the entire city.

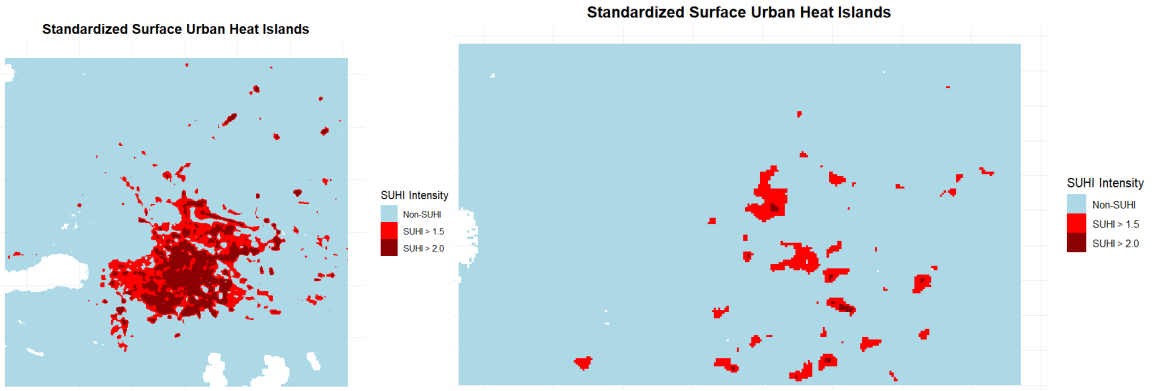

Figure 8. Identification of UHIs based on normalized LST.

Comparing Landsat-based and High-resolution UHI Mapping

The same approaches used to identify UHIs in Landsat images were also applied to the high-resolution thermal data. Using the LST threshold method, the high-resolution image shows a precise distinction between UHIs and non-UHIs, which was not possible with the Landsat datasets. Here, the distinction extends down to street level, providing valuable information for urban planners. When deciding which datasets to use for UHI analysis, the cost of these datasets must also be considered. While comparing the UHI analysis of the high-resolution thermal dataset with the smaller extent of the Landsat dataset, the coarser scale of the latter becomes clearly visible, especially since the dataset was resampled from a resolution of 100m to 30m. However, when comparing the high-resolution data with the combined approach of using a LULC urban mask and LST, more similarities can be observed. The hotspots visible in the urban areas of the Landsat image also appear as clusters of UHIs in the finer resolution. However, it should be noted that some of these areas are actual agricultural land or bare soil, which is a recurring issue. As mentioned above, due to the focus on urban areas in the masked Landsat image, some areas in the city center, such as the airport, are identified as non-UHIs, even though they are clearly recognizable as UHIs in the high-resolution thermal data.

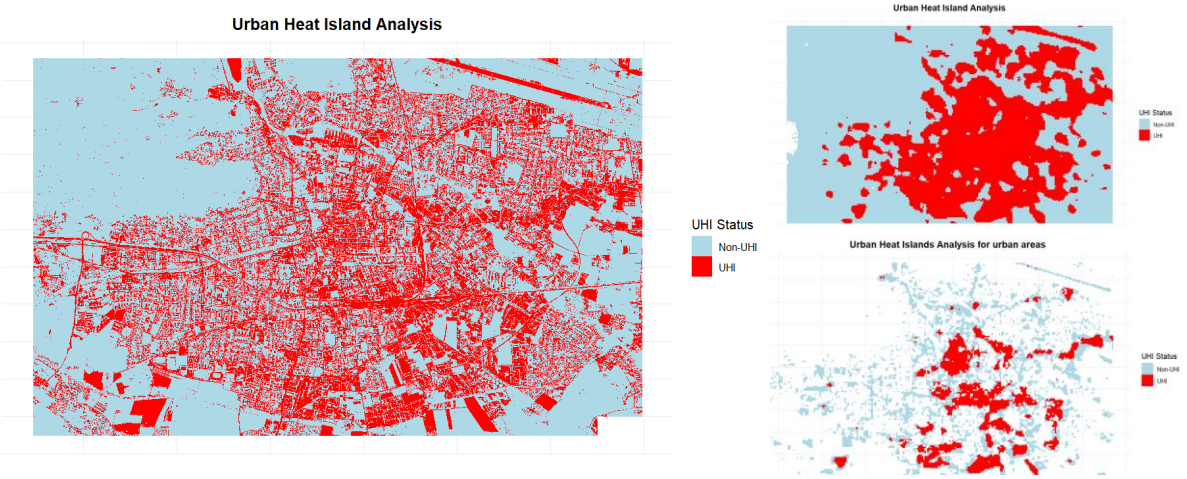

Figure 9. Comparison of UHI identification based on Landsat and high-resolution data.

Additionally, the high-resolution thermal data was acquired not only during the day but also at night during a second flight. Comparing day and night data can provide additional insights into the distribution of UHIs. This could therefore be another advantage of the high-resolution thermal dataset, which must be considered when weighing up freely available and expensive data sources. For the large extent, a finer distribution of the city center can be seen at night, where streets are clearly visible as UHIs. At the same time, bare soil is often identified as UHIs during the day, while these areas appear as non-UHIs during the night. The opposite phenomenon can be seen at lake Wörthersee in the southwest, which is cooler than its surroundings during the day, whereas at night it appears as a UHI due to its water storage capacity.

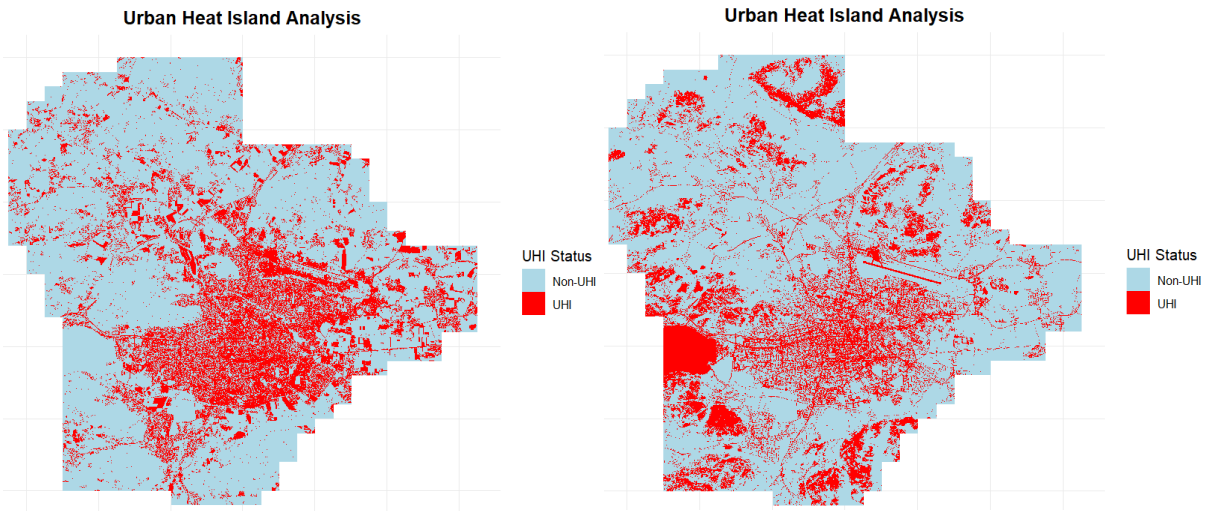

Figure 10. Comparison of UHI identification with high-resolution data during the day and night.

Discussion

To interpret the results efficiently and answer the research questions, it is important to first consider the limitations that arose from the selection of the data and methods presented. Understanding these limitations helps to correctly compare the results with other studies.

Limitations

First, the limitations that arose due to the data should be addressed. As mentioned earlier, the Landsat 9 data was obtained from Landsat Collection 2 Level-2 data, which means that it had already been preprocessed according to ARD standards. For this reason, the LST was not retrieved and calculated using one of the proposed algorithms, but rather the finished product was used. This may have led to some problems, which is why retrieving the LST from DNs should be considered for future research. Here, many similar studies use band 10 and a single channel algorithm (Guechi et al., 2021; Aslan &

Koc-San, 2021; Guha et al., 2018). At the same time, when deriving the spectral indices, some problems arose with values that were completely outside the range due to water and cloud pixels. For this reason, these pixels were masked with the quality assessment band. This is a compromise, as it meant that lake Wörthersee could not be included in the analysis of the Landsat image. However, as mentioned earlier, water bodies often have a positive effect on the microclimate and can contribute to cooler temperatures, which is why they are important for UHI analysis (Guha et al., 2018). For further analysis, consideration should therefore be given to preprocessing the corresponding bands of the spectral indices separately instead of using Landsat Collection 2 Level-2 data or extracting the values of the spectral indices that are outside the range so that water bodies can also be considered.

In addition, there were some limitations because the high-resolution thermal data is currently not calibrated. First, the data could not be projected onto the coordinate reference system of the Landsat dataset, neither could the Landsat dataset be projected onto the correct coordinate system of the high-resolution thermal dataset. Therefore, no true comparison between the two data sources could be made at pixel level. Instead, there was always a slight shift between the two images. Second, especially metallic surfaces, such as the stadium in the southwest of Klagenfurt, mistakenly show lower temperature values than in reality. For a more accurate analysis, it is therefore important to better calibrate the high-resolution thermal data or to mask these misclassified surfaces. At this point, it should be mentioned that similar issues also occurred with Landsat LST, where the stadium is shown with lower LST values and some masked pixels from the quality assessment band, which may be related to the LST estimation with generalized emissivity values and NDVI thresholds. Regarding the methodology, it should be noted that a validation of the LULC classes urban and vegetation has not yet been carried out due to time constraints, but this should be integrated into future research. Nevertheless, the results should be satisfactory for this analysis, as the LULC classification was only used to mask urban areas and the thresholds for identifying the LULC classes were based on existing literature.

Landsat-derived Spectral Indices and LST

In general, the used spectral indices NDVI, SAVI, NDBI and IBI performed well and accurately identified the two LULC classes urban and vegetation. The differences observed between NDVI and SAVI, with a better graduated distinction between vegetation and non-vegetation for SAVI, are consistent with the literature that suggests that SAVI is more accurate than NDVI in detecting less dense vegetation areas (Aslan & Koc-San, 2021). The results of the urban biophysical indices NDBI and IBI are quite similar, which is due to the composition of the IBI, which also takes the NDBI into account. Similarly, the integration of the three spectral indices NDVI, NDBI and MNDWI into the IBI also explains why the

correlation between IBI and LST was the highest of all four spectral indices at 0.669. Although the LULC classification was satisfactory overall, bare soil and urban areas could not be distinguished efficiently, which is a widespread problem in literature. For example, the NDBI cannot sufficiently distinguish between built-up areas and bare soils (Mushore et al., 2021). For this reason, this study used a set of spectral indices, but even then, the problem persisted and bare soils were mostly identified as urban areas.

One of the most frequently studied topics in connection with UHI analysis is the correlation between LST and biophysical indices, as was also investigated in this study. The strong negative correlation between LST and the vegetation biophysical indices is consistent with literature, which states that vegetation absence leads to lower temperatures (Guha et al., 2018; Guechi et al., 2021, Mushore et al., 2021). With regard to the correlation between LST and NDVI in particular, it should be noted that LST was retrieved using generalized NDVI thresholds, which could lead to artificially higher correlations. Furthermore, the observed negative correlation between LST and NDBI as well as IBI has been extensively studied, as built-up areas and bare soil increase surface temperatures (Guha et al., 2018; Guechi et al., 2021, Mushore et al., 2021). Lastly, it should be mentioned that this study only analyzed the correlation for the larger extent of the study area. Since these correlations can vary depending on the spatial scale (Guha et al., 2018), this approach could be considered in future research.

Landsat-based UHI Mapping at Small and Large Spatial Scale

Literature has already analyzed the differences in the detection of UHIs for different spatial scales. For instance, *Guha et al.* (2018) point out that LST correlates differently with spectral indices when considering the whole city or a small area within the city limits. Therefore, these two scales were also considered in this analysis, which provided important insights into the efficiency of methods for identifying UHIs. In general, it was observed that the results for the larger extent were coarser, whereas more differences were visible for the smaller extent. At the same time, the use of the urban mask for UHI analysis helped to distinguish between bare soil and urban areas, as only urban areas were identified as UHIs and bare soils as non-UHIs, especially at the larger extent. Since this is a common problem in UHI analysis using remote sensing data and often cannot be solved with spectral indices alone, the proposed approach could be further investigated in future research. This approach also helped to identify cooler areas in the city in the smaller extent, which can give valuable insights for evidence-based decision making and UHI mitigation strategies, especially with regard to vulnerable groups. This is also consistent with literature suggesting that smaller spatial scales can provide more accurate insights into the distribution of UHIs (Lin et., 2024).

However, it should also be noted that the classification as UHI or non-UHI varied depending on the two different scales for some characteristic areas such as the airport. In the masked UHI analysis, the airport was identified as an UHI in the larger extent and as a non-UHI in the smaller extent, which could lead to some problems that should be addressed in the future. Additionally, the results are currently difficult to verify visually, especially for the standardized LST. To improve the informative value of the visualization, it might therefore be useful to reduce the transparency of the UHI results and interpret them using a meaningful base map.

Comparing Landsat-based and High-resolution UHI Mapping

In general, most studies that identify UHIs use images with medium spatial resolution such as Landsat or images with low spatial resolution from MODIS or Sentinel 3. These results are quite comparable to the results of this study using Landsat 9 data, especially with regard to the aforementioned correlation between LST and spectral indices. When comparing the results from Landsat 9 with the results from the high-resolution thermal data, many differences can be observed. The UHI analysis for the high-resolution thermal data is much more precise and can extend to a street-level, while the results obtained with Landsat 9 only show rough clusters. However, the high-resolution dataset also comes with immense costs, which must be considered in relation to freely available datasets such as Landsat. At the same time, medium spatial resolution and especially low spatial resolution data have the advantage of high temporal coverage, which can also be an important factor when considering multitemporal analysis.

On the other hand, as shown by the results, high-resolution thermal data could be more flexible in terms of time of day. The differences in UHI distribution between day and night can also provide important information for UHI mitigation strategies. However, most studies currently only examine UHIs at a single point in time, so the comparison between day and night as proposed in this study is rather rare (Zhou et al., 2018). Therefore, future research should examine and weigh up the data sources from all angles. After all, the analysis has shown that valuable insights can also be gained from medium-resolution Landsat images, especially when using a combined approach of spectral indices, LULC classification and LST.

Conclusion

In the context of this study, UHIs were identified in Klagenfurt am Wörthersee using medium-resolution Landsat 9 and high-resolution thermal data. The analysis revealed a strong negative correlation between LST and the vegetation biophysical indices NDVI and SAVI, whereas a positive correlation was found between LST and the urban biophysical indices NDBI and IBI. The UHI analysis based on

standardized LST as well as mean LST and its standard deviation showed a clear accumulation of UHIs in the city center. While the larger extent showed the cooling effect of vegetation in the vicinity of Klagenfurt, the smaller extent revealed which surfaces in the city center contribute most to the formation of UHIs. This was particularly evident in the results of the high-resolution thermal dataset, in which the differences between UHIs and non-UHIs extend down to street-level. At the same time, the high-resolution thermal data provided important information about heat distribution in Klagenfurt during day and night. Therefore, this study is highly relevant in the context of ongoing urbanization and climate adaptation, as the results provide city planners with valuable insights for evidence-based decision making.

At the same time, however, it is important to point out the limitations that arose in the context of this study and to make suggestions that could further improve the identification of UHIs in Klagenfurt. First, some problems arose with the data sources for the Landsat 9 data, as pre-processed Landsat Collection 2 Level-2 data was used, while problems with the high-resolution thermal data occurred because the data had not yet been calibrated. These issues should therefore be considered when interpreting the results and should be resolved for future research. In this context, it might be useful to estimate the LST using one of the algorithms proposed in the literature or to add additional data sources such as Sentinel 3 data, as done in a global study by *Sobrino and Irakulis* (2020). Furthermore, as is common in similar studies, only a single day was used for the analysis in this study, but it might also be beneficial to analyze the distribution of UHIs in Klagenfurt using a multitemporal approach that could even consider different seasons (Zhou et al., 2018).Although identifying UHIs using normalized LST, mean LST and its standard deviation was efficient, additional indices could be implemented to better understand the effects of UHIs on the population, such as the Discomfort Index (DI) or the Urban Thermal Field Variation Index (UTFVI), as conducted by *Guha et al.* (2018) or *Sobrino and Irakulis* (2020). Future research could also focus on advanced and more diverse methods that integrate the spatial heterogeneity of UHIs, such as the statistical definition of spatial patterns using spatial autocorrelation as done by *Guo et al.* (2014) and *Bečić and Pažur* (2025) or the use of object-oriented-segmentation of LST as performed by *Guo et al.* (2014). These improved methods could provide results that form an efficient basis for creating more climate-resilient cities.

References & Acknowledgements

Almeida, C. R. d., Teodoro, A. C., & Gonçalves, A. (2021). *Study of the Urban Heat Island (UHI) Using Remote Sensing Data/Techniques: A Systematic Review*. *Environments, 8*(10), Article 105. https://doi.org/10.3390/environments8100105

Aslan, N., & Koc-San, D. (2021). *The use of land cover indices for rapid surface urban heat island detection from multi-temporal Landsat imageries*. *ISPRS International Journal of Geo-Information, 10*(416). https://doi.org/10.3390/ijgi10060416 celiang.tongji.edu.cn+15mdpi.com+15mdpi.com+15

Climate-Data.org. (2025). *Klagenfurt, Carinthia, Austria climate data* [Climate information]. Retrieved July 31, 2025, from https://de.climate-data.org/europa/oesterreich/kaernten/klagenfurt-600/

Earth Resources Observation and Science (EROS) Center. (2020). *Landsat 8-9 Operational Land Imager / Thermal Infrared Sensor Level-2, Collection 2 [dataset]. U.S. Geological Survey*. https://doi.org/10.5066/P9OGBGM6.

FFG – Die Österreichische Forschungsförderungsgesellschaft. (2024). *PROMETHEUS – Progressive methods of thermal high-resolution earth surveillance for urban sustainability*. Retrieved August 9, 2025, from https://projekte.ffg.at/projekt/5121366

Guechi, I., Gherraz, H., & Alkama, D. (2021). *Correlation analysis between biophysical indices and Land Surface Temperature using remote sensing and GIS in Guelma city (Algeria). Bulletin de la Société Royale des Sciences de Liège*, 90, 158–180. https://doi.org/10.25518/0037-9565.10457

Guha, S., Govil, H., Dey, A., & Gill, N. (2018). *Analytical study of land surface temperature with NDVI and NDBI using Landsat 8 OLI and TIRS data in Florence and Naples city, Italy. European Journal of Remote Sensing*, 51(1), 667–678. https://doi.org/10.1080/22797254.2018.1474494

Guo, G., Wu, Z., Xiao, R., Chen, Y., Liu, X. & Zhang, X. (2015). *Impacts of urban biophysical composition on land surface temperature in urban heat island clusters. Landscape and Urban Planning*, 135, 1–10. https://doi.org/10.1016/j.landurbplan.2014.10.002

Huete, A. R. (1988). *A soil-adjusted vegetation index (SAVI)*. Remote Sensing of Environment, 25(3), 295–309. https://doi.org/10.1016/0034-4257(88)90106-X

Lin, X., Cui, Y., Hao, S., Zhu, C., Zhang, P., & Zhao, H. (2024). *Influence of urban landscape pattern on summer surface temperature and its spatial scale effects. Geocarto International*, *40*(1). https://doi.org/10.1080/10106049.2024.2441370

Ma, Y., Kuang, Y., & Huang, N. (2010). *Coupling urbanization analyses for studying urban thermal environment and its interplay with biophysical parameters based on TM/ETM+ imagery. International Journal of Applied Earth Observation and Geoinformation*, 12, 110-118. https://doi.org/10.1016/j.jag.2011.03.010

Magistrat der Landeshauptstadt Klagenfurt am Wörthersee. (2025). *Daten & Fakten – Klagenfurt. Stadtinfo Klagenfurt.* Retrieved July 31, 2025, from https://www.klagenfurt.at/stadtinfo/daten-fakten

Meng, X., Meng, F., Zhao, Z., & Yin, C. (2021). *Prediction of urban heat island effect over Jinan City using the Markov-cellular automata model combined with urban biophysical descriptors. Journal of the Indian Society of Remote Sensing*, 49(4), 997–1009. https://doi.org/10.1007/s12524-020-01274-6

Meteostat. (2025). *Klagenfurt (Austria) weather station historic data* [Weather station data]. Retrieved July 31, 2025, from https://meteostat.net/de/station/11231?t=2024-08-11/2024-08-11

Mushore, T. D., Mutanga, O., & Odindi, J. (2021*). Estimating urban LST using multiple remotely sensed spectral indices and elevation retrievals. Sustainable Cities and Society, 78*, 103623. https://doi.org/10.1016/j.scs.2021.103623

Ritchie, H., Samborska, V., & Roser, M. (2024). *Urbanization*. *Our World in Data*. Retrieved August 9, 2025, from https://ourworldindata.org/urbanization

Rouse, J. W., Haas, R. H., Schell, J. A., & Deering, D. W. (1973). *Monitoring vegetation systems in the Great Plains with ERTS*.

Sangiorgio, V., Fiorito, F., & Santamouris, M. (2020). *Development of a holistic urban heat island evaluation methodology*. *Scientific Reports, 10*, 17913. https://doi.org/10.1038/s41598-020-75018-4

Sobrino, J. A., & Irakulis, I. (2020). *A methodology for comparing the surface urban heat island in selected urban agglomerations around the world from Sentinel-3 SLSTR data*. *Remote Sensing, 12*(2052). https://doi.org/10.3390/rs12122052

Xu, H. (2008). *A new index for delineating built-up land features in satellite imagery*. *International Journal of Remote Sensing*, 29(14), 4269–4276. https://doi.org/10.1080/01431160802039957

Zha, Y., Gao, J., & Ni, S. (2003). *Use of normalized difference built-up index in automatically mapping urban areas from TM imagery. International Journal of Remote Sensing, 24*(3), 583–594. https://doi.org/10.1080/01431160304987

Zhou, D., Xiao, J., Bonafoni, S., Berger, C., Deilami, K., Zhou, Y., Frolking, S., Yao, R., Qiao, Z., & Sobrino, J. A. (2019). *Satellite remote sensing of surface urban heat islands: Progress, challenges, and perspectives*. *Remote Sensing, 11*(1), 48. https://doi.org/10.3390/rs11010048

Acknowledgement of Data Contribution

The high-resolution thermal data used in this study was kindly provided by the PROMETHEUS (Progressive methods of thermal high-resolution earth surveillance for urban sustainability) project and the Paris Lodron University Salzburg. The contribution of their data offered valuable insights and significantly contributed to the outcomes of this research.

Note on the Use of AI and Language Tools

For this essay, ChatGPT was used to organize some ideas into a coherent structure and to improve the sentence structure. DeepL was applied to enhance the language quality by correcting grammatical errors.